Kinetics of the UV-Photopolymerization in TS Diacetylene Single Crystals as Studied by Time Resolved Optical Spectroscopy

H. Niederwald and M. Schwoerer

Physikalisches Institut, Universität Bayreuth, Bayreuth

The intermediate products A, B, C, D, E and V of the UV initiated solid state polymerization in single crystals of 2,4 hexadiynylene bis (p-toluene sulfonate), particulary their kinetics, have been studied by time resolved optical absorption spectroscopy in the temperature range between 180 and 300 K. The description by a simple kinetic model states that A to E react in a direct sequence by monomer addition, which is thermally activated. The activation energies range from 0.25 to 0.30 eV per monomer. At 300 K the reaction rate constants are of the order of $10^6 \, s^{-1}$. − Product V is interpreted as a superposition of several long chain oligomers with reactive carbene chain ends. The reaction V → Polymer is thermally activated with an activation energy of 0,4 eV per monomer. − The fluorescence spectrum of the monomer crystal has been measured for the first time by use of a fast detection system. It is discussed with respect to its significance for the polymerization initiating step. − Deuterium isotope effects on the polymer absorption energy and on reaction kinetics are reported.

Introduction

During the solid state polymerization of disubstituted diacetylenes $(R-C\equiv C-C\equiv C-R)$, single crystals of macroscopic dimensions are converted from their monomer to their highly perfect polymer state [1]. This solid state reaction, schematically shown in Fig. 1, is initiated either by heat or by γ- or UV-irradiation. Both, the mechanical and the optical properties change completely during the topochemical reaction. The monomer crystal is transparent in the visible spectral region and has mechanical properties which are typical for organic molecular crystals. The polymer crystal, however, is extremely anisotropic in several properties. It shows a plane which is highly reflecting and polarizing visible light. This plane contains the polymer chains. Along the chains the tensile strength shows values comparable to those of steel [2].

By far most of the papers on diacetylenes were published during the past 12 years on Wegner's diacetylene, TS i.e. paratoluenesulfonate-oxymethylene substituted diacetylene [3]:

$$R = CH_2O-SO_2-\langle\!\!\!\underset{\cdots}{\bigcirc}\!\!\!\rangle-CH_3 \, .$$
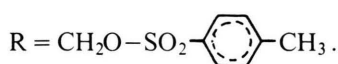
The crystal structures and the structural phase transitions of both, polymer and monomer, are well

known [4−7]. They roughly confirm the early interpretation of Hirshfeld and Schmidt [8] which described "diffusionless polymerization" in a crystal. They statet that "no linear contraction of the stack is needed for polymer formation. For example, a molecule with two unsaturated centers may be so oriented in a stack of identical molecules that it can rotate in place to link up with both its neighbors without any linear displacement of the monomer units so joined." Actually in TS the lattice parameters of monomer and polymer along the polymer chain differ by 4%, the polymer being shorter.

Thermally the reaction is activated with an activation energy of 1 eV/monomer [9]. It is exothermic
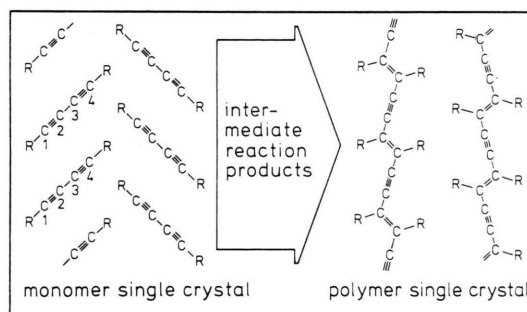

Fig. 1. Reaction scheme of the solid state polymerization of diacetylene single crystals. The monomer crystal reacts after photoinitiation via the intermediate reaction products by 1,4-additions to the perfect polymer crystal. R = side group (see Figure 2).

with a polymerization enthalpy of -1.6 eV/monomer [9]. During the early stages of the thermal polymerization the partially polymerized crystal was described as a solid solution of short polymer chains in the monomer crystal [10]. The structures and dynamics of the intermediates during the pure thermal reaction have been investigated only for very few examples in detail. By ESR, triplet carbenes and biradicals were identified and analyzed [11, 12]. Intermediates in the optical spectrum were not detected, presumably because of their low steady state concentration.

For the UV-initiated reaction at low temperatures (between 4 K and 150 K) a series of photochemically produced intermediates have been investigated by ESR, by ENDOR and by optical spectroscopy [13–25]. In dark all of them were stable at low temperatures; they disappeared at higher temperatures, which are still lower than those which are necessary for the pure dark reaction, and thereby produced polymer.

In order to connect the low temperature photoproducts with the room temperature solid state chemistry we investigated the reaction by UV-flash photolysis: we initiated the reaction by a UV laser flash (310 nm, 15 ns, 1 mJ) and monitored the transient optical spectra at temperatures between 180 K and 300 K. With a monochromatic transient absorption experiment we measured the time evolution of the intermediate products which was then compared to a kinetic model (II).

Besides the absorption transients also a short lived strong monomer fluorescence had been observed which is connected to the initiation reaction (III).

II. Transient Absorption (TA)

1. Experimental

a) Sample Preparation

We investigated TS-crystals, which were perprotonated, perdeuterated, tolyl- or methylene-deuterated, respectively (Figure 2). Crystals were grown from solution by the method of Wegner as described by Huber [26] at a temperature of 20 °C. The small crystals ($6 \times 3 \times 1$ mm^3) were of high crystal quality with low initial polymer concentration of typically 0.02%. Samples were prepared by cleaving the crystals in the (100)-plane. The thick-
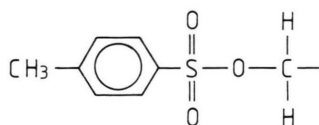
Fig. 2. The paratoluene sulfonate side groups R of TS (see Figure 1).

ness of the slices was between 50 μm and 120 μm. As the perdeuterated crystals showed a significantly higher initial polymer concentration, they had to be cleaved into very thin samples of about 30 μm thickness. For each experiment a fresh sample was used.

b) Monochromatic TA Experiment

The monochromatic TA experiment was performed to measure the time dependence of the optical density (OD) at different wavelengths. The experimental setup is shown in Figure 3. The fresh TS samples were cooled inside the cryostat to temperatures between 4 K and 300 K. The reaction was started by an excimer laser pulse of $\lambda = 308$ nm, 15 ns pulse width and a typical energy of 1 mJ at the surface of the sample (ca. 4 mm^2). Changes in OD were detected by monitoring the transmitted intensity of a cw dyelaser beam with a photodiode. The amplified diode signal was digitized in both, a fast transient digitizer (1 GHz) and a slow transient recorder (2 MHz), respectively. The data were transmitted to a minicomputer for processing. The shutter was controlling the excitation light path as well as the monitor light path. It opened about one millisecond before the reaction was started by the UV-flash. It picked out the regular UV-pulse and prevented the sample to warm up due to monitor light absorption.
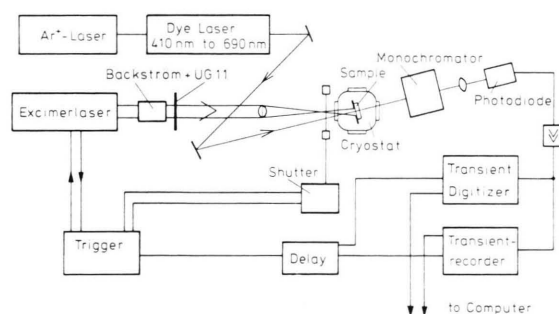
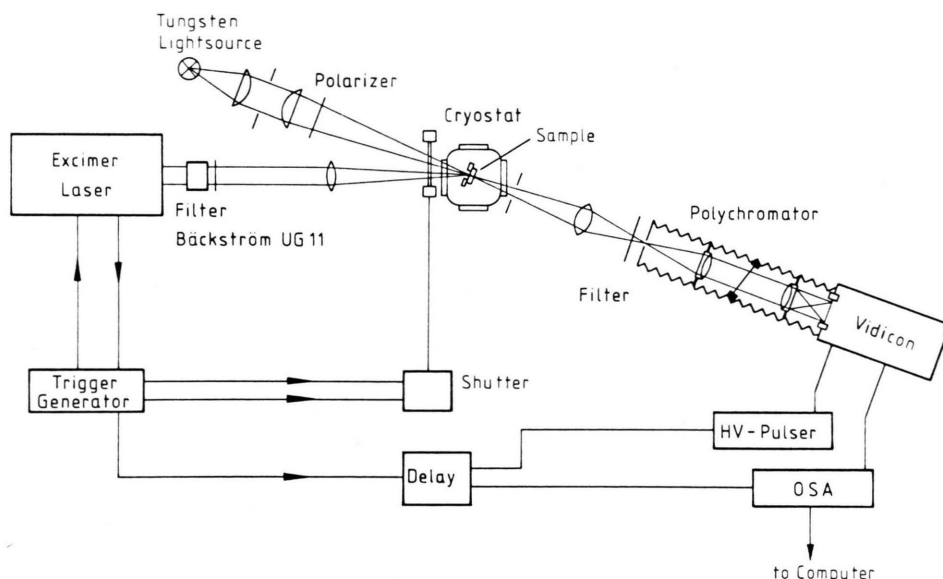Fig. 3. Experimental setup of the monochromatic TA experiment.

Fig. 4. Experimental setup of the polychromatic TA experiment.

c) Polychromatic TA Experiment

The polychromatic TA experiment was setup to measure the transient spectra during the high temperature ($T \gtrsim 180$ K) photopolymerization of TS. Figure 4 shows the experimental setup. The light of a tungsten lamp was polarized and focused onto the sample. The transmitted light was analyzed in a grating polychromator and monitored by a gated vidicon. The polychromator with a grating of 200 lines/mm focussed the whole spectral region from 400 nm to 800 nm onto the target of the vidicon. The gating allowed recording the spectra within a time window of 100 µs. The time resolution was achieved by shifting this time window relative to the reaction initiating UV-pulse by use of a delay unit.

2. Results

By both methods the time development of the solid state photopolymerization after the initiating UV-flash was investigated as a function of sample temperature.

a) Transient Spectra

Figures 5–8 show different states of the reaction. The plotted spectra are difference spectra, i.e. the difference ΔOD between the OD after and before

the initiating UV laser flash. By this method the initial polymer absorption was supressed. Figure 5 shows the difference spectrum within the first 100 µs after the UV-flash at 180 K. For this experiment – and only for this, we accumulated five single flash experiments. This accumulation was necessary because of the low signal to noise ratio due to the short lifetime of the primary photoproducts (A, B, C, D and E).

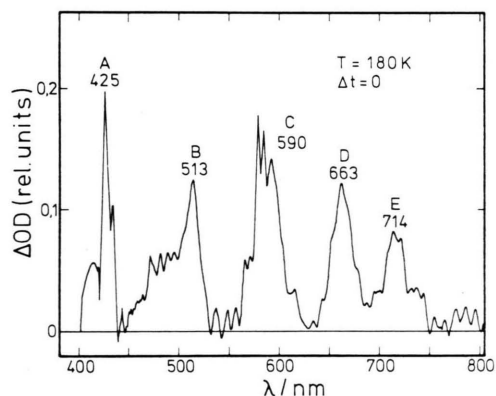The spectra in Figs. 6, 7 and 8 show delayed transient spectra, each recorded from only one single

Fig. 5. Transient difference spectrum of a TS-crystal at 180 K within the first 100 µs after the UV-flash. ΔOD = Difference of the optical densities after and before the UV-flash.
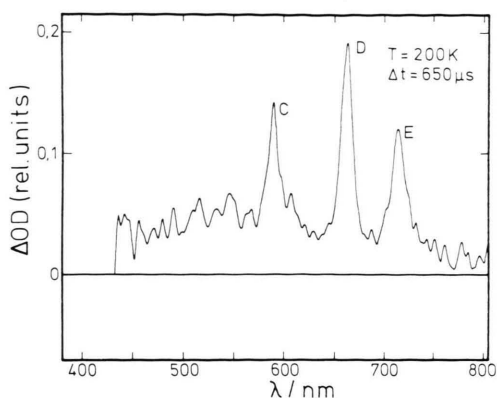
Fig. 6. Transient difference spectrum of a TS-crystal at 200 K within a time window of 100 µs, 650 µs after the UV-flash. The intermediate products A and B have already disappeared.
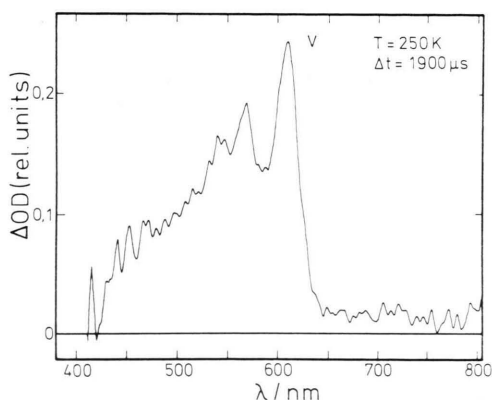

Fig. 7. Transient difference spectrum of a TS-crystal at 250 K, 1.9 ms after the UV-flash, within a time window of 100 µs. Only product V is present. Its absorption structure is very similar to that of the polymer (Fig. 8), but shifted to lower energies.

experiment. Figure 6 was recorded at 200 K, 650 µs after the UV-flash: the products A and B already disappeared. Figure 7 shows a new intermediate product, termed V [27]. It appears significantly later. This spectrum was recorded at 250 K with a delay time of 1.9 ms. Figure 8 shows the spectrum of the same crystal, very long time (500 s) after the UV-flash. It shows the increase of polymer absorption due to the photoreaction. Product V at this time has completely disappeared. Comparison of Figs. 7 and 8 demonstrates the similarity of the absorption bands of product V and the polymer.

Positions and linewidths for the primary intermediate products A to E are within the experi-

mental error, identical with those at low temperature [13]. Product V shows a different behaviour. Its absorption shifts, like that of the polymer [28], to higher energies with increasing temperature.

b) Time Dependence of Intermediates

The time dependence of the concentration of intermediate products in the crystal during polymerization was measured by monitoring the time dependence of ΔOD in the absorption maxima of the different intermediates A, B, C, D and V with the monochromatic TA experiment. Figure 9 shows the time dependence of the cw laser intensity at 514 nm (product B) transmitted by the crystal (T = 250 K) in units of the linear photodiode signal voltage. The signal was simultaneously recorded with the transient digitizer (Fig. 9a) and with the transient recorder (Figure 9b). Figure 9b shows for t < o the opening of the shutter. The monitor laser beam was unblocked within about a quarter of a millisecond. After another half of a millisecond the UV-flash was triggered. In the beginning of the slowly rising polymer absorption the TA of product B is superimposed. The extended time scale in Fig. 9a shows that the absorption maximum of product B was delayed by about 5 µs with respect to the UV-flash. After scale transformation from the signal voltage to ΔOD the transients like the one shown in Fig. 9a were used for the model calculations (see II.2.c). In Fig. 10 the ΔOD of products A,
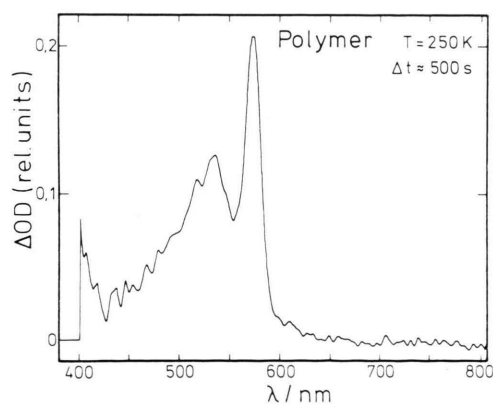

Fig. 8. Stable increase of the optical absorption of the same crystal as in Fig. 7, measured very long time (500 s) after irradiation with the UV-flash. All intermediate products have disappeared, only the UV-generated polymer absorbs. The spectrum is identical with that of a thermally polymerized TS-crystal.
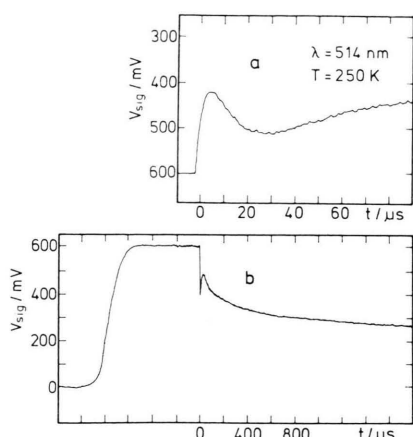
Fig. 9. TA of product B recorded in two different time scales. In Fig. 9b the opening of the shutter is seen, which releases the monitor laser beam within about a quarter of a millisecond. V_{sig} = Signal voltage of the photodiode (see Figure 3).
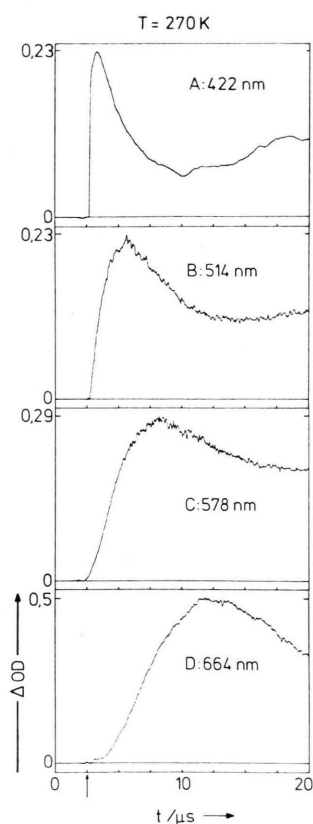

Fig. 10. Time sequence of the intermediate products A, B, C and D at 270 K after the UV-flash which is indicated by an arrow (ΔOD see Figure 5).

B, C, D at 270 K are shown. The time sequence of the intermediates after the UV-flash, which is indicated by an arrow, is obvious.

c) Model calculations

For the model which was used for the interpretation of the experimental data we assumed that the different intermediate products follow one another in a direct sequence. This means, that for each intermediate there is only one important way of generation from its precursor, and only one important way of decay to its successor. Then the time dependence of the optical intermediate absorption bands is described by the following set of rate equations:

$$dn_\alpha/dt = -K_\alpha n_\alpha, \quad dn_A/dt = K_\alpha n_\alpha - K_A n_A, \qquad (1)$$

$$dn_B/dt = K_A n_A - K_B n_B, \quad dn_c/dt = K_B n_B - K_c n_c,$$

$$dn_D/dt = K_c n_c - K_D n_D, \quad dn_E/dt = K_D n_D - K_E n_E.$$

Here n is the concentration of the absorbing intermediate, α indicates the unknown precursor of product A and A, B, C, D and E indicate each of these intermediates, respectively. This model will be discussed now for the intermediate products A to E. The product V shows a more complicated behaviour; it rises much later than E and will be interpreted separately.

If at time $t = t_0$ the precursor α is populated promptly to n_α^0, the solution of these rate equations can be evaluated as follows:

$$n_\alpha = n_\alpha^0 \exp\left(-K_\alpha(t - t_0)\right), \qquad (2)$$

$$n_A = n_\alpha^0 \frac{K_\alpha}{K_A - K_\alpha} \left(\exp\left(-K_\alpha(t - t_0)\right) - \exp\left(-K_A(t - t_0)\right)\right), \qquad (3)$$

$$n_B = n_\alpha^0 \Bigg(\frac{K_\alpha K_A}{(K_A - K_\alpha)(K_B - K_\alpha)} \exp\left(-K_\alpha(t - t_0)\right)$$

$$- \frac{K_\alpha K_A}{(K_A - K_\alpha)(K_B - K_A)} \exp\left(-K_A(t - t_0)\right) \qquad (4)$$

$$+ \frac{K_\alpha K_A}{(K_B - K_A)(K_B - K_\alpha)} \exp\left(-K_B(t - t_0)\right) \Bigg).$$

Furthermore we used the experimental fact that the rise of A, ($\alpha \to$ A), is much faster than all following reactions (Fig. 10), i.e. $K_\alpha \gg K_A, K_B, K_C, K_D$. Then the time dependence of n_B – and of all later inter-

mediates – can be simplified:

$$n_B = n_\alpha^0 \frac{K_A}{K_B - K_A} (\exp(-K_A(t - t_0)) - \exp(-K_B(t - t_0))) ,$$
$$(5)$$

$$n_C = n_\alpha^0 \left(\frac{K_A K_B}{(K_B - K_A)(K_C - K_A)} \exp(-K_A(t - t_0)) \right.$$

$$- \frac{K_A K_B}{(K_B - K_A)(K_C - K_B)} \exp(-K_B(t - t_0)) \quad (6)$$

$$\left. + \frac{K_A K_B}{(K_C - K_B)(K_C - K_A)} \exp(-K_C(t - t_0)) \right) ,$$

$$n_D = n_\alpha^0 K_A K_B K_C \left(\frac{1}{(K_B - K_A)(K_C - K_A)(K_D - K_A)} \right.$$

$$\cdot \exp(-K_A(t - t_0))$$

$$- \frac{1}{(K_B - K_A)(K_C - K_B)(K_D - K_B)}$$

$$\cdot \exp(-K_B(t - t_0))$$

$$+ \frac{1}{(K_C - K_A)(K_C - K_B)(K_D - K_C)}$$

$$\cdot \exp(-K_C(t - t_0))$$

$$- \frac{1}{(K_D - K_A)(K_D - K_B)(K_D - K_C)}$$

$$\left. \cdot \exp(-K_D(t - t_0)) \right) .$$
$$(7)$$

The general formula for the time dependence of the concentration of the intermediate i is:

$$n_i = \sum_{j=1}^{i} a_{ij} \exp(-K_j(t - t_0)) \qquad (8)$$

with

$$a_{ij} = a_{i-1,j} \frac{K_{i-1}}{K_i - K_j} , \quad i, j = A, B, C, D \dots .$$

a_{ii} is evaluated from the initial conditions.

The concentration $n_i(t)$ is proportional to the optical density $\Delta OD_i(t)$ in the absorption of intermediate product i. Thus the formulae ((3) to (7)) can be compared directly with the experimental transients.

This was performed by a least-squares fit program at the computer [27]. As fit parameters were used:

– one amplitude normalizing constant;
– one constant for the linear fit to the slowly rising polymer-absorption which is superimposed to the absorption bands of products A, B and C;

– the rate constants K_A, K_B, K_C and K_D, which finally are the result of the fit operation.

Figure 11 shows as an example for the fits to the different intermediate products both, experimental transient an fit of product C in perdeuterated TS at 200 K. A triexponential fit function according to Eq. (6) was used. As mentioned above the slow rise of polymer absorption was approximated by a straight line. The difference between model and experiment, which indicates the quality of the fit and systematic errors, is plotted around the baseline.

Fits similar to that shown in Fig. 11 were performed for all transients measured at different temperatures and wavelengths – on the whole about 250 different transients and fits. Table 1 shows the numerical values of the time constants (i.e. inverse rate constants) in microseconds. For example for the TA of product D we find τ_{D1}, τ_{D2}, τ_{D3}, τ_{D4}. If our model is appropriate, the following time constants for different photoproducts must be equal:

$$\tau_{A2} = \tau_{B1} = \tau_{C1} = \tau_{D1} = K_A^{-1} ,$$
$$\tau_{B2} = \tau_{C2} = \tau_{D2} \quad\;\; = K_B^{-1} ,$$
$$\tau_{C3} = \tau_{D3} \qquad\;\;\;\; = K_C^{-1} ,$$
$$\tau_{D4} \qquad\qquad\quad\;\; = K_D^{-1} .$$

From Table 1 we can see, that this is in fact true.

Thus our simple kinetic model states, that the intermediates are indeed produced in a direct sequence, from A to E:

$$A \xrightarrow{K_A} B \xrightarrow{K_B} C \xrightarrow{K_C} D \xrightarrow{K_D} E \dots .$$
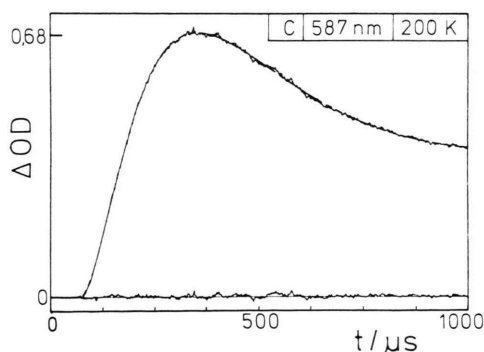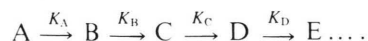

Fig. 11. Experimental transient and model curve for product C in perdeuterated TS at $T = 200$ K. The model curve includes the triexponential function of Eq. (6) which describes product C and, superimposed, the linear fit to the slow rise of the polymer absorption. Around the baseline the residuum (difference between experiment and model) is plotted.

Table 1. Time constants for different intermediate products in perprotonated (h) and perdeuterated (d) TS crystals, evaluated from model fit calculations.

Time Constants/μs			Temperature/K					
			295	270	250	230	200	180
A (422 nm)	h	τ_{A1}				< 0.1		
		τ_{A2}	1 ± 0.2	2.6 ± 0.5	6 ± 1	18 ± 3	160 ± 40	630 ± 100
	d	τ_{A1}				< 0.1		
		τ_{A2}	0.9 ± 0.2	2.2 ± 0.5	4.5 ± 1.5	11 ± 2	115 ± 20	600 ± 50
B (514 nm)	h	τ_{B1}	0.9 ± 0.5	2.6 ± 1.5	5 ± 2	18.5 ± 8	160 ± 80	400 ± 200
		τ_{B2}	1.0 ± 0.5	2.5 ± 1.5	7 ± 3	16 ± 8	120 ± 70	1300 ± 500
	d	τ_{B1}	0.8 ± 0.5	1.5 ± 0.7	4 ± 2	12 ± 5	110 ± 30	400 ± 200
		τ_{B2}	0.7 ± 0.4	2.5 ± 0.8	6.5 ± 3	19 ± 6	100 ± 30	800 ± 300
C (587 nm)	h	τ_{C1}	0.9 ± 0.5	2.6 ± 1	6 ± 3	15 ± 7	120 ± 60	400 ± 200
		τ_{C2}	0.9 ± 0.5	2.4 ± 1	6 ± 3	15 ± 7	150 ± 70	1000 ± 500
		τ_{C3}	1.25 ± 0.6	3.0 ± 1.5	14 ± 7	30 ± 15	400 ± 200	2000 ± 1000
	d	τ_{C1}	0.9 ± 0.4	1.7 ± 0.8	5 ± 2	12 ± 5	90 ± 40	400 ± 200
		τ_{C2}	0.9 ± 0.4	1.7 ± 0.8	4.5 ± 2	12 ± 5	100 ± 50	800 ± 400
		τ_{C3}	1.5 ± 0.7	5.7 ± 2.5	15 ± 7	44 ± 20	300 ± 150	1500 ± 700
D (664 nm)	h	τ_{D1}	1 ± 0.5	2.5 ± 1	6 ± 3	13 ± 6	100 ± 50	
		τ_{D2}	1 ± 0.5	2.5 ± 1.5	6 ± 3	13 ± 6	200 ± 100	
		τ_{D3}	1 ± 0.5	2.5 ± 1.5	7 ± 3	24 ± 10	400 ± 200	
		τ_{D4}	2 ± 1	7 ± 3	25 ± 10	60 ± 20	400 ± 200	
	d	τ_{D1}	0.9 ± 0.4	1.6 ± 0.5	5 ± 2.5	12 ± 4		
		τ_{D2}	0.6 ± 0.3	1.6 ± 0.6	5 ± 2.5	12 ± 4		
		τ_{D3}	1 ± 0.4	3.3 ± 1.5	7 ± 3	14 ± 5		
		τ_{D4}	2.4 ± 1	6.2 ± 2	16 ± 5	50 ± 20		
V (610 nm)	h	τ_{V1}	60 ± 30	230 ± 110	$(1 ± 0.4)10^3$	$(3 ± 1)10^3$		
		τ_{V2}	730 ± 100	$(3.3 ± 0.5)10^3$	$(1.25 ± 0.25)10^4$	$(8 ± 3)10^4$	$(1.5 ± 0.5)10^6$	
	d	τ_{V1}	65 ± 30	≲ 300		≲ 4 · 10^3		
		τ_{V2}	$(7 ± 2)10^3$	$(5 ± 1)10^4$		$(1.5 ± 0.5)10^6$		

The slow product V shows a complicated time behaviour and does not follow this simple sequence. A biexponential model was fitted to the transient of V to get numerical values for rise and decay-time of the absorption.

In Table 1 we see, that V rises significantly slower than the first products, and the decay is again slower by one order of magnitude. The time for the decay of product V is identical with that for the rise of the polymer absorption. Especially at room temperature our experimental results agree with those of Leyrer and Wegner [29] who measured the rise of polymer absorption at room temperature in a polycrystalline sample. Product V is therefore interpreted as the direct precursor of the polymer: the prepolymer.

In Fig. 12 the temperature dependencies of three rate constants are plotted. They are very well described by an Arrhenius law:

$$K = K_0 \exp(-\Delta E / kT).$$

From plots like that in Fig. 12 activation energies ΔE for the reactions and the preexponential frequency factors K_0 are evaluated. These are shown in Table 2. For the reaction A → B we find $\Delta E = 0.25 ± 0.03$ eV per monomer. The activation energies for the following reaction steps are almost equal, with a slight increase of about 2% for each step. The activation energy for the decay of product V is 0.40 ± 0.03 eV/monomer.

The preexponential frequency factors K_0 were estimated by extrapolation of the temperature
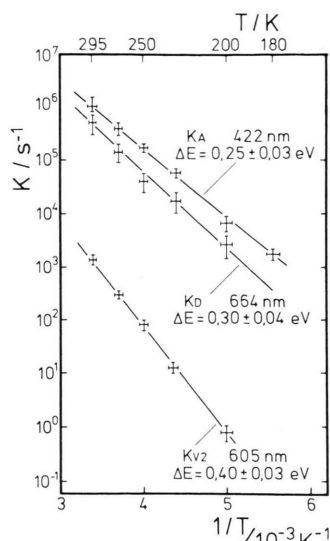
Fig. 12. Temperature dependencies of the rate constants for the decays of products A, D and V. They are described by Arrhenius laws, in a range of three orders of magnitude.

Table 2. Activation energies ΔE and frequency factors K_0 for the reaction rates, evaluated from their Arrhenius plots.

	K_A	K_B	K_C	K_D	K_{V2}
ΔE/eV	0.25 ± 0.03	0.26 ± 0.03	0.30 ± 0.04	0.30 ± 0.04	0.40 ± 0.03
K_0/s^{-1}	$10^{10 \pm 1}$	$10^{11 \pm 1}$	$10^{11 \pm 1}$	$10^{11 \pm 1}$	$10^{10 \pm 1}$

dependencies. These estimated values are strongly dependent on the activation energy. Within error margins of one order of magnitude the frequency factors for all reactions are about 10^{11} s^{-1}.

III. Fluorescence of the TS Monomer Crystal

1. Experiment

For the observation of the fluorescence spectra the detection system of the polychromatic transient absorption experiment was used. It was rotated by 90° relative to the UV-excitation beam in order to avoid absorption of the emitted light by the initial polymer within the crystal. With this setup it was possible to record the complete emission spectrum between 400 and 800 nm after a single UV-flash, which was provided by the XeCl Excimer Laser. We were able to observe for the first time the fluorescence spectrum of a monomer TS crystal. Earlier

efforts which used conventional emission spectroscopy failed, because the crystal surface polymerizes very quickly under UV-irradiation at wavelengths shorter than 330 nm [30]. The lifetime of the fluorescence was measured with a fast PIN-diode, the excitation light was discriminated by filters.

2. Results: Lifetime and Spectra

The fluorescence lifetime is shorter than 10 ns. The fluorescence pulse line shape is exactly the same like that of the excitation UV-pulse ($\tau = 15$ ns). Figure 13 shows the fluorescence spectrum of a monomer TS-crystal at 10 K. It is broad, without structure and red-shifted by about 10 000 cm^{-1} with respect to the excitation energy. This spectrum was accumulated from 20 single spectra, each excited by one single UV-pulse on the surface of the same crystal. This procedure was shown not to affect the shape of the spectrum. From a different experiment in which we detected the overall fluorescence intensity using different longpass-filters in the detection light path, we know that the contribution to the fluorescence in the region between 308 nm and 400 nm is less than 5%.

The absence of structure was not caused by the poor resolution of the detection system which was about 5 nm. The fluorescence intensity decreases with increasing temperature. At room temperature it was about one order of magnitude weaker, but still detectable. A temperature dependence of the fluorescence band shape was not observed.

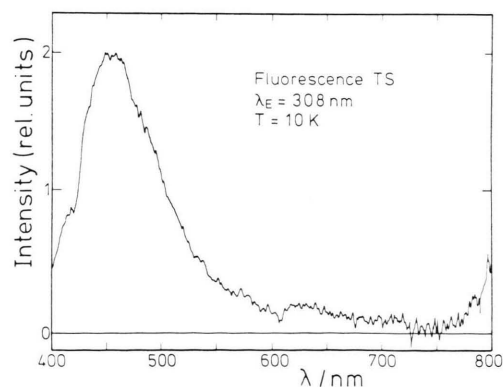Besides this "monomer crystal fluorescence" a "defect fluorescence" was observed which also de-

Fig. 13. Fluorescence spectrum of a TS crystal ($T = 10$ K) after flash excitation at $\lambda = 308$ nm.
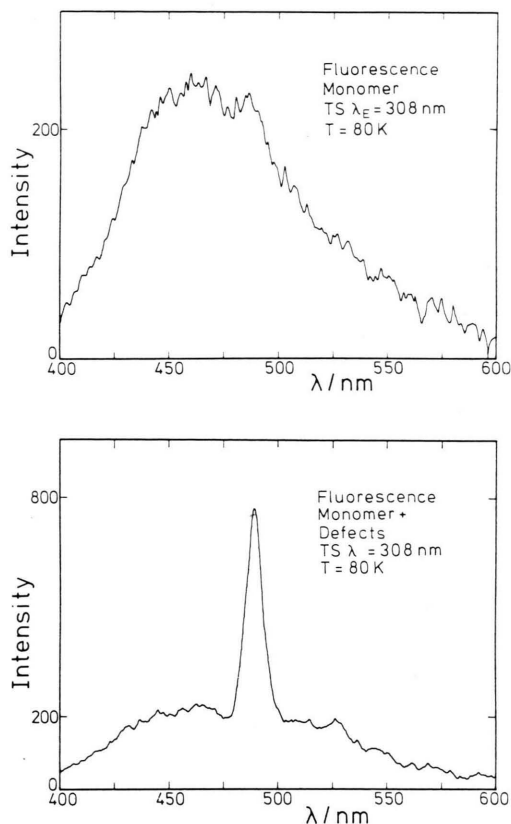
Fig. 14. Fluorescence spectrum of a good quality crystal (Fig. 14a) and of a badly grown crystal with many defects (Figure 14b). Comparison of the intensity scales shows that the monomer crystal fluorescence is not quenched by the defect fluorescence.

creased with increasing polymer content (Figure 14b). These defect states have also been observed in emission by Eichele after excitation at lower energies than in our experiment [30] and in absorption by Bloor and Preston [28]. (From the experiments of Eichele we know that the defect emission shows a more detailed structure than the spectrum shown in Figure 14b. This difference is only due to the poor resolution of our detection system.) The defect fluorescence is strongest in badly grown

Fig. 15. Biradical dimer.

crystals. They show many small splits parallel to the c-axis of the crystal. Figure 14b shows the fluorescence spectrum of such a bad crystal and Fig. 14a that of a high quality crystal under the same experimental conditions at 80 K. By comparing the intensity scales we see that the crystal emission is not quenched by the defect emission. From this we conclude that there is no excitation transport to the defect centers.

IV. Discussion

1. Chain Propagation

The results of Chapt. II show that the simple model

$$A \xrightarrow{K_A \Delta E_A} B \xrightarrow{K_B \Delta E_B} C \xrightarrow{K_C \Delta E_C} D \xrightarrow{K_D \Delta E_D} E$$

describes the reaction very well. The intermediate products are produced directly from one another. All reactions show nearly the same activation energy, the same reaction rate constant and the same isotope effect (see Chapt. V). This allows the conclusion, that each step is the addition of one monomer unit. As photoproduct A rises directly from the photoexcitation of the monomer, it is most probably the dimer. Thus the intermediates are the dimer (A), the trimer (B), the tetramer (C), the pentamer (D) and the hexamer (E). These results confirm the earlier conclusions of Sixl et al. [14, 19].

The difference between the individual addition reactions is the fact, that the monomer is linked to an oligomer which for each step is one monomer unit longer than for the preceeding step. This can explain the observed slight increase of the activation energy for longer oligomers, because of the 4% reduction of the length of the oligomer repeat unit as compared to the monomer lattice parameter b [6]. Thus the distance between the oligomer head and the next nearest monomer increases with increasing oligomer length. Therefore a higher amount of energy is needed to bring the neighbouring monomer into its critical reaction distance.

The increase in activation energies also agrees with the results of annealing experiments after low temperature UV irradiation [19, 20]: Each intermediate product is stable at a slightly higher temperature than its precursor. The frequency factors K_0 are all of the order of $10^{11}\,s^{-1}$. They are — within an experimental error of one order of magni-
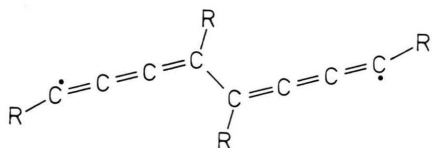
tude – equal for each reaction step. This indicates that each reaction step is driven by the same type of vibration. We assume the probability for the chemical reaction between neighbouring monomer and oligomer to be one within one period of this vibration at infinite temperature. This implies that the molecules do react if the vibrational amplitude is high enough to bring the reacting atoms closer together than a critical reaction distance. Then the K_0-factor is equal to the frequency of this reaction driving vibration.

$10^{11}\,s^{-1}$ is a frequency which is too low for intramolecular vibrations usually observed. At this frequency acoustic phonons and low energy optical phonons are to be expected. Schott et al. [31], measured phonon dispersion curves of TS by inelastic neutron scattering. They observed an optical phonon at very low frequency of about $10^{11}\,s^{-1}$ at the boundary of the brillonin zone. This actually could be the monomer addition driving vibration.

2. Electronic structure of the intermediate products

From ESR experiments [19], bleaching experiments [18], model calculations [32], kinetic data, and from the isotope effects to be described in Chapt. V it is known, that the intermediates A, B, C, D, E have biradical structure (Figure 15). From the completely different behaviour of product V (Kinetics, isotope effect, optical absorption at higher energy than its precursor) it is obvious, that its electronic structure must be different.

Comparing to ESR experiments of Huber et al. [15] and of Neumann [20] we conclude that V is the absorption band of different dicarbenes (DC) and longchain carbenes (LC) (see Figure 16). We assume their absorption bands to be superimposed
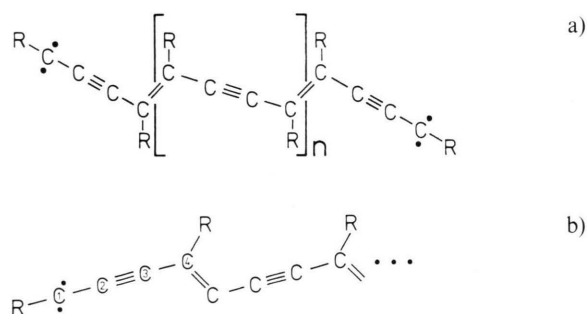

Fig. 16. Bicarbene (Fig. 16a) and asymmetric carbene (Figure 16b).

because these intermediates are long chain oligomers [25], which all absorb at an energy close to the value for infinite chain length. In diacetylene oligomer chains the convergence to this value should be reached at shorter lengths than for a one dimensional free electron model because the excitation is not extended over the whole chain length. Calculations of Cade and Movaghar [33] show that the exciton is limited to about six monomer units.

The stable polymer absorbs at a still higher energy than its precursor, product V. The structural change that leads to this experimental fact should be the reaction from the carbene chain end to a chemically stable chain end.

Thus, the lifetime of product V can be interpreted as the lifetime of the reactive chain end. This lifetime determines, together with the monomer addition time, the kinetic chain length defined as the number of polymerized diacetylene monomers per one initiation event. We conclude:

i) As the carbene lifetime τ_{V2} in perdeuterated TS is ten times longer than in protonated TS (see Chapt. V), the kinetic chain length in d-TS should be significantly longer than in h-TS. This has direct influences on both, the polymer yield under UV irradiation [27, 34] and on the time dependence of the thermal polymerization [34]:

(1) The polymer yield P is the product of the Quantum yield Q for the initiation event and the kinetic chain length L:

$$P = Q \cdot L \,.$$

So P is higher for d-TS than for h-TS [27].

(2) The autocatalytic region during the thermal polymerization of TS starts at a critical conversion of about 10%; assuming identical thermal chain initiation rates for d-TS and for h-TS, the longer kinetic chain length in d-TS causes this critical conversion to be reached earlier in d-TS than in h-TS, as it was observed by Kröhnke [34].

ii) Because carbene decay (τ_{V2} of Table 1) and monomer addition (e.g. τ_{D4} of Table 1) have different activation energies, the kinetic chain length should increase with decreasing temperature. From Table 1 follows:

$$\left.\frac{\tau_{V2}}{\tau_{D4}}\right|_{200\,K} = 10 \cdot \left.\frac{\tau_{V2}}{\tau_{D4}}\right|_{295\,K} \,.$$

Indeed we observed in preliminary experiments [27], that the polymer yield increases with decreasing temperature.

3. Fluorescence and Initiation Reaction

The fluorescence observed in TS seems to be typical for diacetylene crystals. For comparison we show in Fig. 17 two examples: the fluorescence spectra of the diacetylenes HDD and DAH, excited by 310 nm UV irradiation [30]. All spectra show the same features: A broadband emission, no structure and a strong red-shift relative to excitation. DAH and HDD however have completely different photochemical properties than TS:

- DAH is not photoreactive under UV-light;
- in HDD some photoreactions occur, but no photopolymerization.

From the observed red-shift we conclude a strong molecular rearrangement, following the excitation, similar to the formation of an excimer [35]. This rearrangement occurs within less than 10^{-8} s.

Because the emission is typical for diacetylenes, the "diacetylene backbone" of the monomer mole-
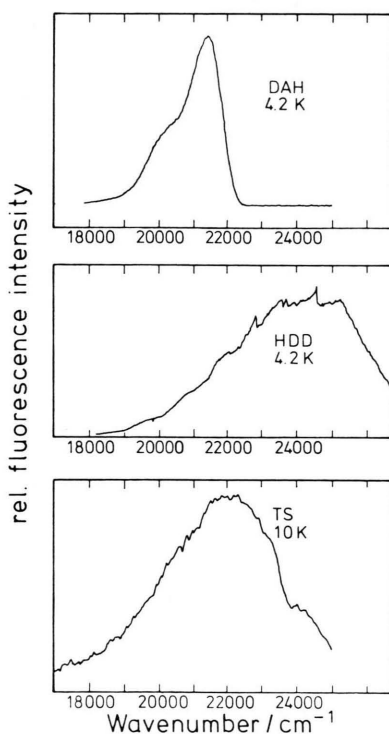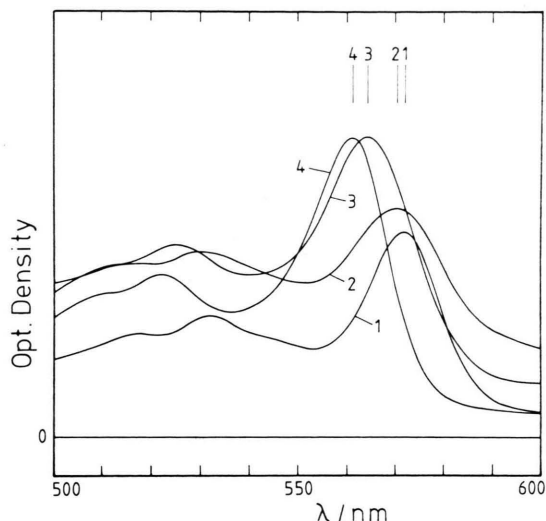
Fig. 18. Shift of the polymer absorption due to deuteration. 1: perprotonated TS; 2: tolyl deuterated TS; 3: methylene deuterated TS; 4: perdeuterated TS. The spectra were recorded at room temperature.

cule must be involved in the absorption, the rearrangement and the emission. The side-groups seem to be less involved in these processes. However, their influence on the following chemical processes is strong.

As the fluorescence is strong and the quantum yield for dimer formation is less than 10^{-3} [27, 36] we believe that fluorescence emission is the most probable path of desactivation for the singulet excited TS monomer molecule and that dimer formation is a concurring process which needs an additional phonon or a molecular vibration to take place. This is also indicated by the nonlinear intensity dependence of dimer formation which was observed by Neumann and Sixl [14].

V. Isotope effects

1) Spectra

The influence of deuteration on the electronic excitation energies is remarkably different for the first intermediate product absorptions (A, B, C, D, E) and for the polymer absorption, respectively: the shift of the absorption maxima of the first intermediates is negligible (less than 3×10^{-3}). That of the polymer absorption is strong (Fig. 18); deuteration leads to higher excitation energies. The most

Fig. 17. Fluorescence spectra of DAH and HDD ($T = 4.2$ K, $\lambda_{exc} = 310$ nm) [30] and of TS ($T = 10$ K, $\lambda_{exc} = 308$ nm). The crystal emission in the three systems is broad without structure and strongly red shifted with respect to the excitation.

important contribution is due to deuteration of the methylene groups which are situated close to the polymer backbone. Perdeuterated crystals show the strongest blue-shift of $300 \, cm^{-1}$ at room temperature. It is temperature dependent; the 80 K value is $140 \, cm^{-1}$.

The blue shift in absorption due to deuteration is not new for organic crystals; for example the $T_1 \leftarrow S_0$ transition in perdeuterated naphthalene shifts by $100 \, cm^{-1}$ to higher energies as compared to the protonated crystal [37]. The blue shift can be explained qualitatively using the fact of the lower zero point energy of the deuterated molecule and assuming that the potential for the normal vibrations is softer in the excited electronic state as compared to the ground state. Actually Batchfelder and Bloor [38] measured the force constants for some normal modes in the excited electronic state of PTS and found that most of them are significantly smaller than in the ground state.

2) Kinetic isotope effects

The numerical results are contained in Table 1. We find completely different isotope effects in the reaction kinetics for the first intermediate products A to E and for the decay of the prepolymer V, respectively.

For the first reactions: $A \rightarrow B$, $B \rightarrow C$, $C \rightarrow D$ and $D \rightarrow E$ we get

$$0.8 \lesssim K_H/K_D \lesssim 1$$

where K_H is the rate constant for the protonated and K_D that for the deuterated system.

This is a weak inverse secondary kinetic isotope effect of the second kind, following the nomenclature of Streitwieser [39].

The direction and magnitude of this kinetic isotope effect seems to be determined by the change in hybridization of the reacting carbon atom from sp to sp^2 during the addition of one monomer unit to short oligomers. Such relations between change in hybridization and kinetic isotope effects were reported for similar reactions by Pryor et al. [40].

For the reaction V $\rightarrow$ Polymer we find

$$K_H/K_D \approx 10 \, .$$

This is an extremely high secondary isotope effect. Usually values between 0.5 and 2 are observed [41]. The reaction V $\rightarrow$ Polymer was interpreted as the change from the reactive carbene chain end to stable polymer head (see Chapt. IV 2). This is an electronic rearrangement within the polymer head including for example singlet triplet intersystem crossing. For these processes strong isotope effects have been reported: for example the (radiationless) triplet lifetime of Perdeutero-Naphthalene is about 7 times longer than the triplet lifetime of Naphthalene [42].

[1] G. Wegner, Z. Naturforsch. **24 b**, 824 (1969).
[2] R. H. Baughman, H. Gleiter, and N. Senfeld, J. Polym. Sci. Polym. Phys. Ed. **13**, 1871 (1975).
[3] see for example D. Bloor, Developments in Crystalline Polymers, Ed. D. C. Basset, Applied Science Publishers, London 1982.
[4] D. Kobelt and E. F. Paulus, Acta Crystallographica **B 30**, 232 (1974).
[5] V. Enkelmann, Acta Crystallographica **B 33**, 2842 (1977).
[6] V. Enkelmann and G. Wegner, Angew. Chem. **89, 6**, 432 (1977).
[7] D. Bloor, L. Koski, G. C. Stevens, F. H. Preston, and D. J. Ando, J. Nat. Science **10**, 1678 (1975).

[8] F. L. Hirshfeld and G. M. J. Schmidt, J. Poly. Sci. **A 2**, 2181 (1964).
[9] G. N. Patel, R. R. Chance, E. A. Turi, and Y. D. Khanna, J. Am. Chem. Soc. **100**, 6644 (1978).
[10] R. H. Baughman and R. R. Chance, Ann. NY Acad. Sci. **313**, 705 (1978).
[11] R. Huber, Thesis, Universität Bayreuth 1981.
[12] H. Eichele, M. Schwoerer, R. Huber, and D. Bloor, Chem. Phys. Lett. **42**, 342 (1976).
[13] H. Sixl, W. Hersel, and H. C. Wolf, Chem. Phys. Lett. **53, 1**, 39 (1978).
[14] W. Neumann and H. Sixl, Chem. Phys. **50**, 273 (1980).

[15] R. Huber and M. Schwoerer, Chem. Phys. Lett. **73, 1,** 10 (1980).
[16] R. Huber, M. Schwoerer, H. Benk, and H. Sixl, Chem. Phys. Lett. **78, 3,** 416 (1981).
[17] M. Schwoerer, R. Huber, and W. Hartl, Chem. Phys. **55, 1,** 97 (1981).
[18] C. Bubeck, W. Hersel, W. Neumann, H. Sixl, and J. Waldmann, Chem. Phys. **51,** 1 (1980).
[19] C. Bubeck, H. Sixl, and W. Neumann, Chem. Phys. **48,** 269 (1980).
[20] W. Neumann and H. Sixl, Chem. Phys. **58,** 303 (1981).
[21] C. Bubeck, H. Sixl, and H. C. Wolf, Chem. Phys. **32,** 231 (1978).
[22] C. Bubeck, H. Sixl, D. Bloor, and G. Wegner, Chem. Phys. Lett. **63, 3,** 574 (1979).
[23] R. Huber, M. Schwoerer, C. Bubeck, and H. Sixl, Chem. Phys. Lett. **53,** 35 (1978).
[24] H. Niederwald, H. Eichele, and M. Schwoerer, Chem. Phys. Lett. **72, 2,** 242 (1980).
[25] W. Hartl and M. Schwoerer, Chem. Phys. **69,** 443 (1982).
[26] R. Huber, Diploma Thesis, Universität Stuttgart 1976.
[27] H. Niederwald, Thesis, Universität Bayreuth 1982.
[28] D. Bloor and F. H. Preston, Phys. stat. sol. (a) **40,** 279 (1977).
[29] R. J. Leyrer and G. Wegner, Ber. Bunsenges. Phys. Chem. **83,** 470 (1979).
[30] H. Eichele, Thesis, Universität Bayreuth 1978 and H. Eichele and M. Schwoerer, Phys. stat. sol. (a) **43,** 465 (1977).
[31] M. Schott, private communication, to be published.
[32] H. Sixl, H. Gross, and W. Neumann, to be published.
[32]a) H. Gross and H. Sixl, to be published.
[33] N. A. Cade and B. Movaghar, to be published.
[34] C. Kröhnke, Thesis, Universität Freiburg 1980.
[35] T. Förster, Angew. Chem. **81, 10,** 364 (1969).
[36] H. Niederwald, K.-H. Richter, W. Güttler, and M. Schwoerer, Laser Chem. 1983 to be published.
[37] H. Port and H. C. Wolf, Z. Naturforsch. **23a, 2,** 315 (1968).
[38] D. N. Batchelder and D. Bloor, J. Phys. C: Solid State Phys. **15,** 3005 (1982).
[39] Streitwieser jr., Ann. NY Acad. Sci. **84,** 576 (1960).
[40] W. A. Pryor, R. W. Henderson, R. A. Patsiga, and N. Carroll, J. Amer. Chem. Soc. **88, 6,** 1199 (1966).
[41] E. A. Halevi, Secondary Isotope Effects, Prog. Phys. Org. Chem. **1,** 109 (1963).
[42] C. A. Hutchison and B. W. Maugum, J. Chem. Phys. **34,** 908 (1961).